

## KILL LINE MODEL CROSS FLOW INLINE COUPLED VORTEX-INDUCED VIBRATION

**Baiheng Wu**

Department of Mechanical Engineering  
MIT  
Cambridge, MA, USA  
Email: wbh@mit.edu

**Jorlyn Le Garrec**

Department of Mechanical Engineering  
MIT  
Cambridge, MA, USA  
Email: jlegarre@mit.edu

**Dixia Fan**

Department of Mechanical Engineering  
MIT  
Cambridge, MA, USA  
Email: dfan@mit.edu

**Michael S. Triantafyllou**

Department of Mechanical Engineering  
MIT  
Cambridge, MA, USA  
Email: mistetri@mit.edu

### ABSTRACT

*Currents and waves cause flow-structure interaction problems in systems installed in the ocean. Particularly for bluff bodies, vortices form in the body wake, which can cause strong structural vibrations (Vortex-Induced Vibrations, VIV). The magnitude and frequency content of VIV is determined by the shape, material properties, and size of the bluff body, and the nature and velocity of the oncoming flow. Riser systems are extensively used in the ocean to drill for oil wells, or produce oil and gas from the bottom of the ocean. Risers often consist of a central pipe, surrounded by several smaller cylinders, including the kill and choke lines. We present a series of experiments involving forced in-line and cross flow motions of short rigid sections of a riser containing 6 symmetrically arranged kill and choke lines. The experiments were carried out at the MIT Towing Tank. We present a systematic database of the hydrodynamic coefficients, consisting of the forces in phase with velocity and the added mass coefficients that are also suitable to be used with semi-empirical VIV predicting codes.*

### INTRODUCTION

Vortex-induced vibrations are generated as oncoming fluid flow interacts with a flexible body or structure. In the classical case of a flexibly mounted rigid cylinder, alternating vortices

form on either side of the bluff body causing it to vibrate. This phenomenon can lead to the aeolian tones in the wind, or to fatigue damage in larger ocean structures. The potential for fatigue damage is one of the main motivations for research on VIV [1].

Systematic experiments have generated a substantial databases of VIV coefficients to predict the effect on a variety of structural systems [2, 3]. A drilling riser consists of a larger-diameter pipe containing the drilling string, and stretching from the well at the sea floor to the surface structure. The purpose of the riser is to protect the drilling string and also return the circulating mud back to the surface [4]. The kill line pumps kill fluid such that fluid can then flow through the choke line to the surface. Both of these lines are high-pressure pipes essential for maintaining fluid pressure in the riser. These lines run along the outside of the central riser from the bottom of the sea floor to the surface, creating a specific cross-sectional shape that is also subject to VIV. In order to accurately model VIV, databases have been compiled of various structural shapes, based on rigid cylinder experiments, and are utilized in semi-empirical programs, such as Shear7 (Vandiver 1999) [5], VIVA (Triantafyllou 1999) [6], and VIVANA (Larsen 2000) [7]. These programs are widely used in industry and for research purposes today. To ensure that these programs are kept up to date and relevant to structures regularly used today, it is important to compile databases specific to the structures studied. Previous research shows that VIV is depen-

dent on various factors, but the shape of the body and the characteristics of the oncoming fluid flow are the most significant ones [8]. The work presented in this paper focuses on the VIV coefficients of risers with kill & choke lines.

### EXPERIMENTAL PARAMETERS AND MODEL SETUP

All experiments were conducted in the MIT Towing Tank, using a special small tank equipped with a velocity-controlled towing carriage that rides along the top of the tank. The length of the tank is 2.5 meters while the effective length is 1.5 meters. The width of the tank is 0.9 meters. All experiments were conducted as forced oscillatory motions while towing the model along two orthogonal tracks. An ATI 6-Axis Force transducer is used to measure the forces.

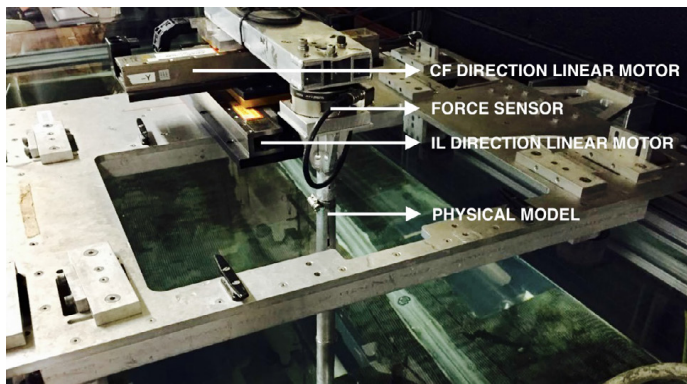


FIGURE 1: EXPERIMENT APPARATUS

A single kill line model was used in all experiments. The model consisted of a single central riser and 6 equally spaced kill lines, located around the central riser. The central riser to kill line diameter ratio is 3 to 1.



FIGURE 2: KILL LINE MODEL IN EXPERIMENTS

The geometrical parameters of the kill line riser are shown in Fig 1b.  $D$  denotes the diameter of the inner drilling riser;  $d$  the diameter of the outer kill and choke lines (all outer lines have the same diameter).  $D/d$  is the ratio of inner to outer diameter of the model. The three geometric parameters are listed below:

- $D$ : diameter of inner drilling riser
- $d$ : diameter of kill and choke lines

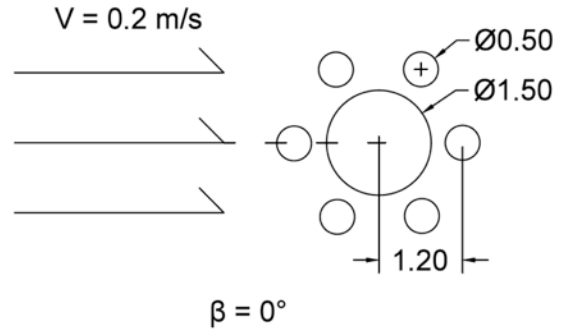


FIGURE 3a. FLOW-INCIDENT ANGLE IS 0°

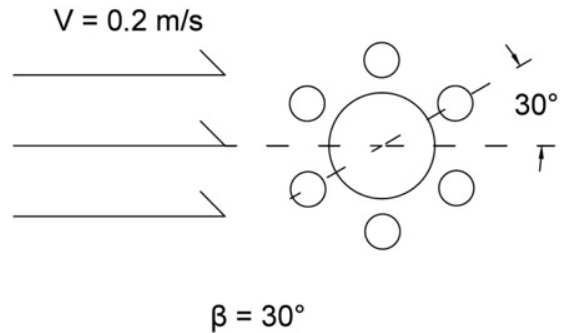


FIGURE 3b. FLOW-INCIDENT ANGLE IS 30°

FIGURE 3: KILL LINE ORIENTATION RELATIVE TO DIFFERENT FLOW-INCIDENT ANGLES

$D/d$ : ratio of inner to outer diameter of the model

The equations of motion are provided in equations (1) and (2).  $y$  is the cross-flow (CF) motion;  $x$  is the in-line (IL) motion,  $A_y$  is the amplitude of the CF motion;  $A_x$  is the amplitude of the IL motion,  $\omega_y$  is the circular frequency of the CF motion;  $\omega_x$  is the circular frequency of the IL motion, which is usually twice  $\omega_y$ , and  $\theta$  is the phase angle of the IL and CF motion. During tests, the value of  $\theta$  is valued from 0 to  $7\pi/4$  with steps of  $\pi/4$ .

$$y = A_y \sin(\omega_y t) \quad (1)$$

$$x = A_x \sin(\omega_x t + \theta) \quad (2)$$

A main parameter is the reduced velocity,  $U_r$ , defined as:

$$U_r = \frac{U}{fD} \quad (3)$$

where  $U$  is the velocity of the flow,  $f$  is the frequency of oscillation, and  $D$  is the riser diameter.  $U_r$  is valued at 6 or 8 in each experiment.

The dimensionless parameters,  $A_y D$  and  $A_x D$  provide the amplitude of vibration divided by the riser diameter  $D$ , in the CF and IL directions, respectively:

$$A_y D = \frac{A_y}{D} \quad (4)$$

$$A_x D = \frac{A_x}{D} \quad (5)$$

$A_y D$  is the series: 0, 0.15, 0.3, 0.5, 0.75 and 1 and  $A_x D$  is the series: 0, 0.05, 0.1, 0.15 and 0.3.

The hydrodynamic coefficients calculated and compiled in a database from the experiments are:

- $C_d$ : Mean drag force coefficient
- $C_{lv}$ : Lift force coefficient in velocity phase
- $C_{dv}$ : Drag force coefficient in velocity phase
- $C_{my}$ : Added mass coefficient in CF motion
- $C_{mx}$ : Added mass coefficient in IL motion

## RESULTS OF EXPERIMENT

This section provides the hydrodynamic coefficients recorded:  $C_d$ ,  $C_{lv}$ ,  $C_{dv}$ ,  $C_{my}$ ,  $C_{mx}$ . Areas that are split by a darker black line signify a shift from negative to positive coefficient values. Positive values of the force coefficients in phase with velocity correspond to energy transfer from the surrounding fluid to the structure, resulting in VIV; whereas negative values indicate damping in the system.

Figures 4a and 4b show  $C_d$  values for phase angles  $0^\circ$  and  $30^\circ$ . At  $U_r = 6$  and phase  $0^\circ$ ,  $C_d$  is largely independent of the amplitude of motion in the X direction, while it depends strongly on the amplitude in the Y direction; this trend, however, changes at the higher reduced velocity  $U_r = 8$ , where dependence on both amplitudes is noted. The results at phase  $30^\circ$  are similar. Overall, forces stay in the negative range, indicating damping in the system.

Figure 5 shows  $C_d$  values for both  $0^\circ$  and  $30^\circ$  with reduced velocity of 6 and  $\theta$  of  $135^\circ$ .  $C_d$  values for  $0^\circ$  are usually larger than for  $30^\circ$  at the same  $A_x D$  and  $A_y D$ ; but the overall trend is consistent between the two cases.

Figures 6a and 6b show similar trends between  $0^\circ$  and  $30^\circ$  for the  $C_{lv}$  coefficients.  $C_{lv}$  is weakly dependent on the amplitude of motion in the X direction and depends strongly on the amplitude in the Y direction. In both cases, there are positive values present in the reduced velocity of  $U_r = 8$ . While positive values are attained across all X direction amplitudes for both cases, the model at  $30^\circ$  shows more positive values for increasing amplitude in the Y direction. For the results of Figure 6b, the  $30^\circ$  model had one kill line out front, which may have caused it to respond closer to a single cylinder. This can also explain why the system is able to become excited at lower X directional amplitudes than the  $0^\circ$  model.

Figure 7 shows the  $C_{lv}$  values for both  $0^\circ$  and  $30^\circ$  with reduced velocity of 8 and  $\theta$  of  $225^\circ$ . We find that positive values for  $30^\circ$  are larger than for  $0^\circ$ .

Figures 8a and 8b show the results of  $C_{dv}$  coefficients for all experiments for the kill line at  $0^\circ$  and  $30^\circ$ . In both cases the results follow similar trends. It is noted that  $C_{dv}$  depends strongly on the amplitude in the X direction. Both cases continue with

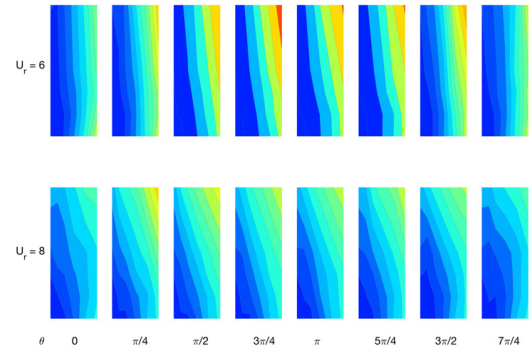


FIGURE 4a. FLOW-INCIDENT ANGLE IS  $0^\circ$

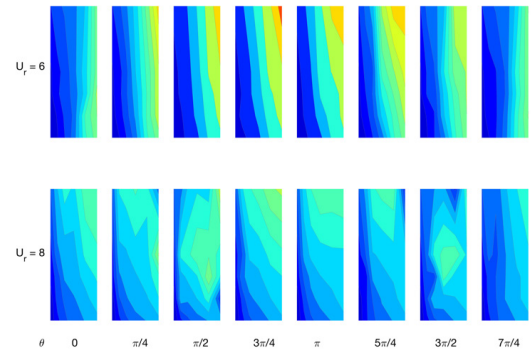


FIGURE 4b. FLOW-INCIDENT ANGLE IS  $30^\circ$

FIGURE 4: SERIES OF CONTOURS OF ALL  $C_d$  VALUES OF THE KILL LINE MODEL

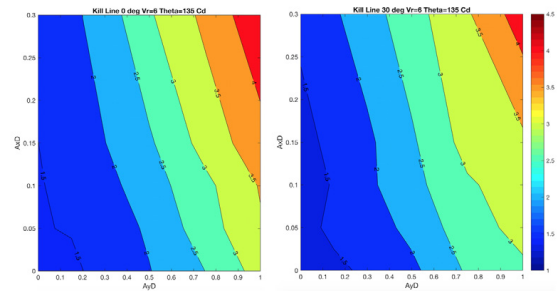


FIGURE 5: COMPARISON OF  $C_d$  AT  $U_r=6$  AND  $\theta=135^\circ$

the same trend for both reduced velocities, 6 and 8. In both cases positive values occur at high Y direction amplitudes combined with low X direction amplitudes. This shows that the system becomes most excited as it moves mainly in the cross flow direction.

Figure 9 shows the  $C_{dv}$  values for both  $0^\circ$  and  $30^\circ$  with reduced velocity of 6 and  $\theta$  of  $135^\circ$ . We find higher positive values in the case of  $30^\circ$  than in  $0^\circ$ , however, but the overall trend is

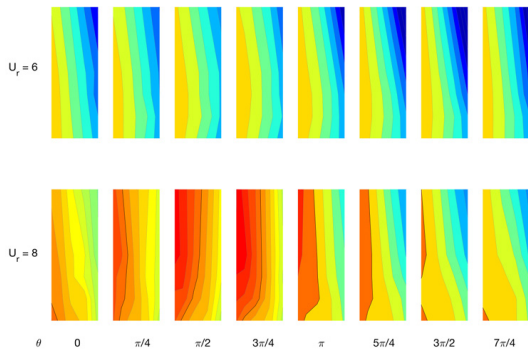


FIGURE 6a. FLOW-INCIDENT ANGLE IS 0°

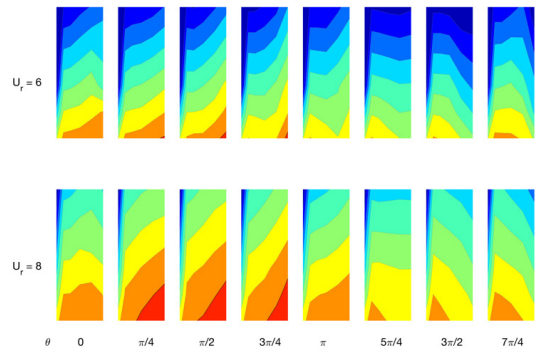


FIGURE 8a. FLOW-INCIDENT ANGLE IS 0°

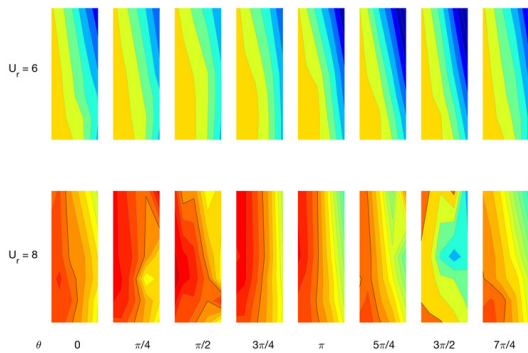


FIGURE 6b. FLOW-INCIDENT ANGLE IS 30°

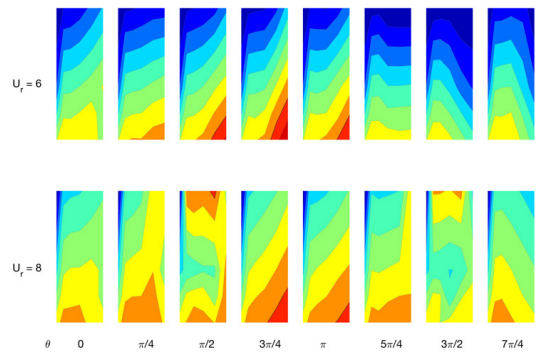
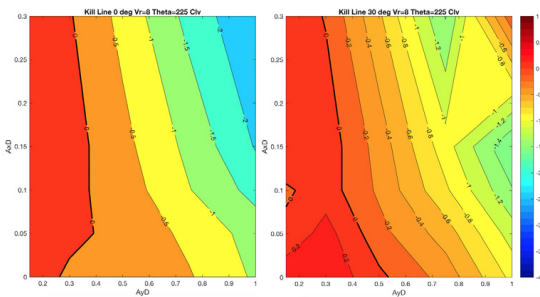


FIGURE 8b. FLOW-INCIDENT ANGLE IS 30°

**FIGURE 6:** SERIES OF CONTOURS OF ALL  $C_{lV}$  VALUES OF THE KILL LINE MODEL

**FIGURE 8:** SERIES OF CONTOURS OF ALL  $C_{dV}$  VALUES OF THE KILL LINE MODEL



**FIGURE 7:** COMPARISON OF  $C_{lV}$  AT  $U_r=8$  AND  $\theta=225^\circ$

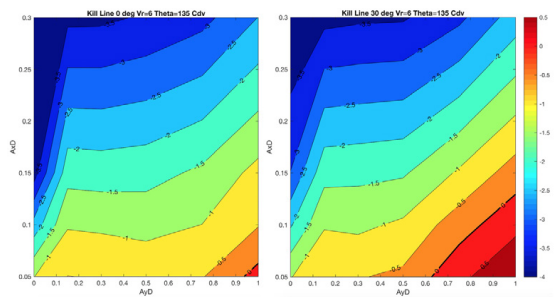


**FIGURE 9:** COMPARISON OF  $C_{dV}$  AT  $U_r=6$  AND  $\theta=135^\circ$

similar in the two cases.

Figures 10a and 10b show the results for the  $C_{mX}$  coefficients at 0° and 30°, showing much stronger dependence on the Y amplitude. The values are positive almost throughout the reduced velocities and phase angles, reaching values of up to positive 5. This shows that the system is subject to substantial added mass in the in-line direction.

Figure 11 shows the  $C_{mX}$  values for both 0° and 30° with

reduced velocity of 8 and  $\theta$  of 45°.  $C_{mX}$  does not exhibit any persistent trend. The graph of 30° shows an unusual case of negative  $C_{mX}$  coefficients. The graph of 0°, on the other hand, remains positive, averaging around a value of 3.4.

Figures 12a and 12b show results for the  $C_{mY}$  coefficients at 0° and 30°. This case does not show any persistent trend. Initially,  $C_{mY}$  appears to remain high, with a value around 4 for most cases. However, as the reduced velocity increases to 8, and

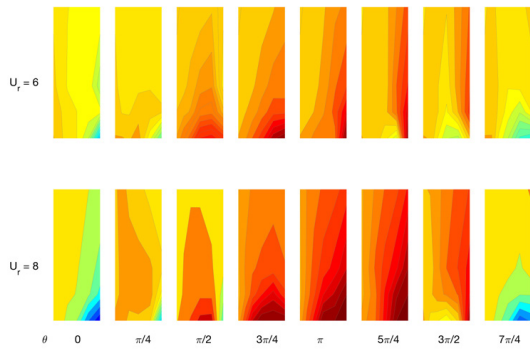


FIGURE 10a. FLOW-INCIDENT ANGLE IS 0°

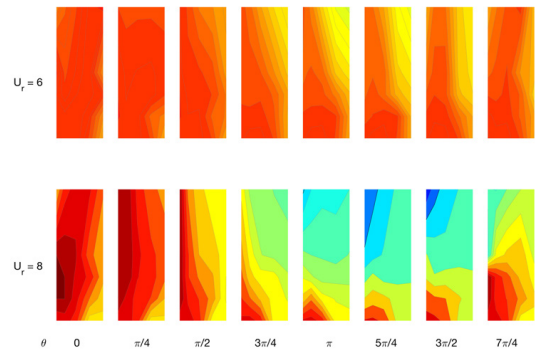


FIGURE 12a. FLOW-INCIDENT ANGLE IS 0°

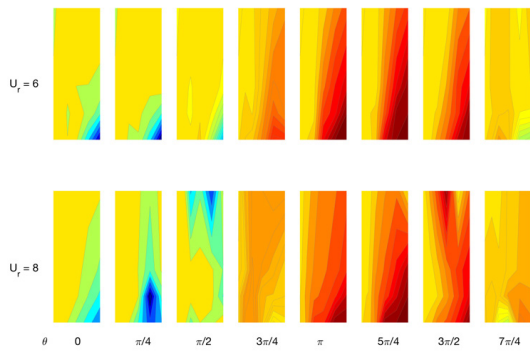


FIGURE 10b. FLOW-INCIDENT ANGLE IS 30°

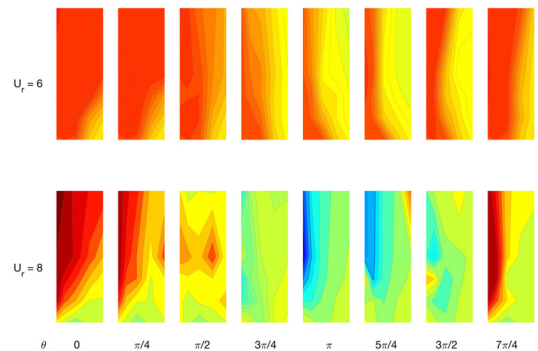


FIGURE 12b. FLOW-INCIDENT ANGLE IS 30°

FIGURE 10: SERIES OF CONTOURS OF ALL  $C_{m_x}$  VALUES OF THE KILL LINE MODEL

FIGURE 12: SERIES OF CONTOURS OF ALL  $C_{m_y}$  VALUES OF THE KILL LINE MODEL

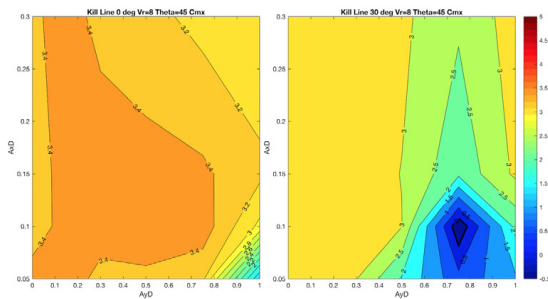


FIGURE 11: COMPARISON OF  $C_{m_x}$  AT  $U_r=8$  AND  $\theta=45^\circ$

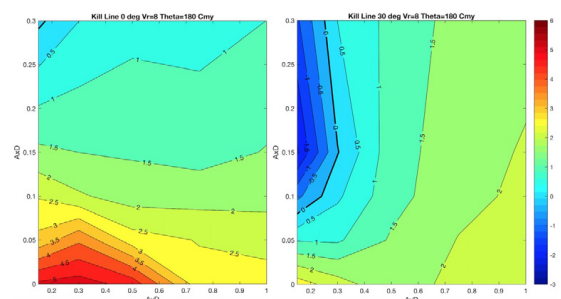


FIGURE 13: COMPARISON OF  $C_{m_y}$  AT  $U_r=8$  AND  $\theta=180^\circ$

the phase angle increases, this values decreases. Interesting cases are found for phase angles of  $\pi$ ,  $5\pi/4$ , and  $3\pi/2$ , where the added mass becomes negative.

Figure 13 shows the  $C_{m_y}$  values for both  $0^\circ$  and  $30^\circ$  with reduced velocity of 8 and  $\theta$  of  $180^\circ$ .  $C_{m_y}$  values show different trends for each case. The graph of  $30^\circ$  shows an unusual case of negative  $C_{m_y}$  coefficients. The graph of  $0^\circ$ , on the other hand, remains positive, reaching values of 5.

## CONCLUSION

Hydrodynamic databases are a tool for the offshore system designer to calculate the fatigue damage caused by vortex-induced vibrations. Herein we described a comprehensive hydrodynamic database for a riser configuration with six kill lines that had a 3 to 1 ratio of central riser to external kill line diameters, undergoing forced in-line and cross-flow vibrations within an oncoming stream. The key hydrodynamic coefficients of lift force

in phase with cross-flow velocity, drag force in phase with in-line velocity, and the two added mass coefficients, were recorded and analyzed. Results of these experiments show that hydrodynamic coefficients for the model at incident angles of  $0^\circ$  and  $30^\circ$ , have similar trends and take comparable values. Positive force coefficients, which indicate transfer of energy from the flow to the vibrating structure, and hence self-sustained VIV, are prevalent; and take larger values for the  $30^\circ$  configuration than for the  $0^\circ$  case. Added mass coefficients for both the in-line and cross-flow directions reach values as high as 5, hence altering the natural frequencies of the structure, particularly for mass ratios close to 1.

## REFERENCES

- [1] Xu, Y., Fu, S., Chen, Y., Zhong, Q., and Fan, D., 2013. "Experimental investigation on vortex induced forces of oscillating cylinder at high reynolds number". *Ocean Systems Engineering*, 3(3), pp. 167–180.
- [2] Gopalkrishnan, R., 1993. "Vortex-induced forces on oscillating bluff cylinders". No. WHOI-92-38, WOODS HOLE OCEANOGRAPHIC INSTITUTION, MA.
- [3] Zheng, H., 2014. "The influence of high harmonic force on fatigue life and its prediction via coupled inline-crossflow viv modeling". PhD Diss., Massachusetts Institute of Technology, Cambridge, MA.
- [4] Guesnon, J., Gaillard, C., and Richard, F., 2002. "Ultra deep water drilling riser design and relative technology". *Oil Gas Science and Technology*, 57(1), pp. 39–57.
- [5] Vandiver, J. Kim and Li, L., 2005. *SHEAR7 V4.4 Program Theoretical Manual*. MIT, Cambridge, MA.
- [6] Triantafyllou, Michael, 2015. *VIVA: programs for calculating riser vortex induced oscillations and fatigue life*. Testing Tank Facility, Massachusetts Institute of Technology, Cambridge, MA.
- [7] Larsen, Carl M. and Lie, H. and Passano, E. and Yttervik, R. and Wu, J. and Baarholm, G., 2009. *VIVANA - Theory Manual*. Marintek, Trondheim, Norway.
- [8] Le Garrec, J., Fan, D., Wu, B., and Triantafyllou, M. S., 2016. "Experimental investigation of cross flow-inline coupled vortex-induced vibration on riser with finite length buoyancy module". *OCEANS 2016 MTS/IEEE Monterey*, pp. 1–7.